Journal of Korea Multimedia Society Vol. 17, No. 8, August 2014(pp. 1012-1019)
http://dx.doi.org/10.9717/kmms.2014.17.8.1012

# Bandwidth-Efficient Precoding Scheme for Downlink Smart Utility Networks

B.W. Kim†

## ABSTRACT

The emerging smart utility networks (SUN) provide two-way communications between smart meters and smart appliances for purpose of low power usage, low cost, and high reliability. This paper deals with a bandwidth-efficient communication method based on the hidden pilot-aided scheme using a precoder in downlink SUN suitable for high-rate multimedia applications. With the aid of the design of a precoder and a superimposed hidden pilot, it is possible to estimate the channel without loss of bandwidth. In the channel estimation procedure, the inevitable data interference, which degrades the performance of channel estimation, can be reduced by the precoder design with an iterative scheme. Computer simulations show that the proposed scheme outperforms the conventional method in terms of achievable data rate, especially when a large number of subcarriers are employed.

**Key words:** Smart Utility Networks, Precoding, Bandwidth Efficiency

## 1. INTRODUCTION

The increasing interest in modern smart grid requires a new technology for providing the two-way communication between the consumer and the utility at the appliance/meter level [1-6]. This will enable the consumer to continuously monitor power usage and make instantaneous decisions to control electric devices at consumers' homes or offices to reduce energy usage, cost and increase service reliability. Smart utility networks (SUN), a subordinated network in the smart grid, consist of smart home appliances and meters equipped with radio terminals. Smart devices in SUN can automatically control power consumption during peak and offpeak load times according to the demand requirement. This will ensure that power is not utilized by the appliance when the cost of power consumption is expensive. In addition, SUN may support other functionality needs, such as multimedia data transmission from substations to smart devices in addition to normal control data.

IEEE 802.15.4g specification for Physical Layer (PHY) is built for smart devices of SUN [7]. Among the various alternative PHY designs, multi-rate and multi-regional orthogonal frequency division multiplexing (MR-OFDM) was designed to provide higher data rates in channels that have significant delay spread. Due to the fast growth of demands on multimedia services of smart devices, SUN are expected to support high data rate applications. In addition, in order to reduce the power consumption and interference during communications between smart devices, a transmission method to shorten transmission time is required. To solve these problems, multiple-input multiple-output (MIMO) systems can be a viable solution for high data rate communications over SUN. As the downlink of the SUN with dense smart meters will act as the bottleneck link, an ef-

※ Corresponding Author : Byung Wook Kim, Address: (712-701) 50, Gamasil-gil, Hayang-eup, Gyeongsan-si, Gyeongsangbuk-do, Korea, TEL : +82-53-600-5524, FAX : +82-53-600-5539 , E-mail : bwkim@kiu.kr

Receipt date : Apr. 25, 2014, Revision date : Jun. 13, 2014
Approval date : Jul. 2, 2014
† School of Electrical and Railway Engineering, Kyungil University

ficient usage of downlink wireless resources is important to provide high quality of communication services.

In the wireless SUN, a pilot-symbol-aided modulation (PSAM) scheme, one of the most widely used schemes in cellular systems, can be used to estimate the channel state information (CSI) exploiting pilot symbols that are previously known at the user terminal [8]. Accurate channel estimates can be obtained by using the judiciously placed pilots [9], whereas it consumes bandwidth which is valuable in wireless communications. Although blind channel estimation [10] offers a bandwidth-efficient method exploiting statistical and other properties of the data, it has its inherent shortcomings, such as slow convergence and phase ambiguity. An alternative method is the superimposed training (ST) scheme [11-12] has a virtue of no loss in information rate at the expense of data power. However, this method may degrade the performance of channel estimation due to the effect of inherent interference of data. Use of a hidden pilot based precoding scheme can be a feasible solution to this problem, as it removes inevitable unknown data interference with the aid of the design of a precoding and a ST sequence [13].

In this paper, we propose a bandwidth efficient precoding scheme for downlink SUN for achieving high data rates. Considering different designs of a precoder and a superimposed hidden pilot per transmit antenna in smart devices, spatially multiplexed data can be successfully recovered. In addition, due to the spreading effect of the information data over the total available bandwidth using a precoder, it is possible to provide high frequency diversity. The performance gain of achievable data rate becomes significant when a large number of subcarriers is employed.

This paper is organized as follows. In Section 2, a system model of the proposed scheme is introduced. Section 3 presents the channel estimation and symbol detection. The results of computer simulations are shown in Section 4. Finally, conclusions are drawn in Section 5.

## 2. SYSTEM MODEL OF A HIDDEN PILOT-AIDED PRECODING SCHEME

### 2.1 MR-OFDM system model

We consider a downlink transmission from an access point, such as a coordinator or a router, equipped with two transmit antennas, to $K$ smart devices, such as in-home and metering devices, also having two receive antennas, depicted in Fig. 1. At each transmit antenna, a MR-OFDM modulator followed by the proposed hidden pilot aided

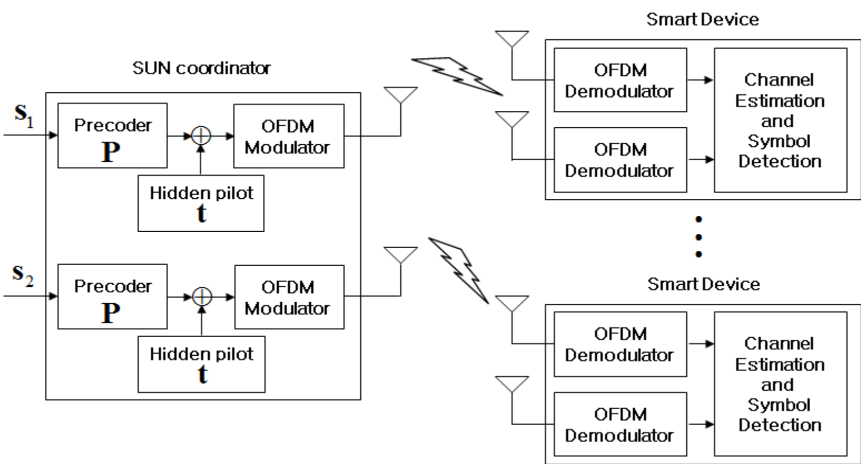


Fig. 1. The downlink smart utility network.

precoder is used. Let $N$ be the total number of subcarriers in one OFDM symbol. Remind that application of block transmission with a cyclic prefix (CP) over a time-dispersive channel can be modeled as transmission over a channel with a circulant channel matrix. And the length of the CP $L$ is set to be equal to the number of non-zero taps of the impulse response for each channel.

After removing the CP at the $k'$-th smart device's $i$-th receive antenna, we obtain an $N\times 1$ vector $\bar{\boldsymbol{r}}_i^{k'}$, which can be written as

$$\bar{\boldsymbol{r}}_i^{k'} = \sum_{j=1}^{2} \boldsymbol{H}_{ji}^{k'}\left(\sum_{k=1}^{K} \boldsymbol{F}_1^H \boldsymbol{U}_j^k\right) + \bar{\boldsymbol{n}}_i^{k'},\ i=1,2 \tag{1}$$

where $\boldsymbol{U}_j^k = [U_j^k(0), U_j^k(1), ..., U_j^k(N-1)]^T$ is an $N\times 1$ precoded transmit symbol block for the $k$-th assigned device, from the $j$-th transmit antenna. $\boldsymbol{H}_{ji}^{k'}$ is the $N\times N$ downlink channel matrix, which is a circulant matrix with the first column given by $[\boldsymbol{h}_{ji}^{k'T}, 0, ..., 0]^T$, and $\boldsymbol{h}_{ji}^{k'} = [h_{ji}^{k'}(0), h_{ji}^{k'}(1), ..., h_{ji}^{k'}(L-1)]^T$ is the $L\times 1$ vector representing the length $L$ channel impulse response from the coordinator's $j$-th transmit antenna to the $i$-th receive antenna of the $k'$-th smart device. The $N\times N$ discrete Fourier transform (DFT) matrix $\boldsymbol{F}_1$ has an $(m,n)$ entry $(1/\sqrt{N})e^{-j2\pi mn/N}$, $m,n = 0,1,...,N-1$. We assume that $\bar{\boldsymbol{n}}_i^{k'} = [\bar{n}_i^{k'}(0), \bar{n}_i^{k'}(1), ..., \bar{n}_i^{k'}(N-1)]^T$ is additive white Gaussian noise (AWGN), whose elements are independent and identically distributed (i.i.d.) zero mean complex Gaussian random variables with variance $\sigma_{\boldsymbol{n}}^2$.

### 2.2 Design of a precoder and a superimposed hidden pilot

In this subsection, we derive the design of a proposed scheme based on a precoder and a ST symbol. Since a training sequence for channel estimation is simply added to the precoded data, there exists mutual interference between them. To mitigate inherent mutual interference, the precoder based on orthogonal polyphase sequences [13], which have good periodic autocorrelation and crosscorrelation properties, is exploited. These properties are utilized to eliminate the interference between the data and the hidden pilot guaranteeing almost no loss of transmit data rate. To generate these sequences, the length of a sequence is set to $p^{r-1}$, where $p$ is prime and $r(>1)$ is an integer. Then, the $N/2K-1$ $(=p^{r-1})$ numbers of polyphase sequence sets such that $\boldsymbol{C} = [\boldsymbol{c}_0, \boldsymbol{c}_1, ..., \boldsymbol{c}_{N/2K-2}]$, where $\boldsymbol{c}_i = [c_i(0), c_i(1), ..., c_i(N/2K-2)]^T$, can be generated by

$$c_i(n) = \frac{1}{\sqrt{\dfrac{N}{2K-1}}} exp\left(j2\pi\left[\frac{v(n)}{p} + \frac{i\times n}{\dfrac{N}{2K-1}}\right]\right). \tag{2}$$

Then, we can split the polyphase sequence sets into two parts, the sequence for a precoder and for a hidden pilot. Design of the precoder matrix $\boldsymbol{P}$ and the pilot vector $\boldsymbol{t}$ can be expressed as follows:

$$\begin{aligned} \boldsymbol{P} &= \boldsymbol{F}_2 \cdot [\boldsymbol{c}'_0, \boldsymbol{c}'_1, ..., \boldsymbol{c}'_{N/2K-3}] \\ \boldsymbol{t} &= \boldsymbol{F}_2 \cdot \boldsymbol{c}'_{N/2K-2}, \end{aligned} \tag{3}$$

where $\boldsymbol{c}' = [\boldsymbol{c}^T 0]^T$ is an $N/2K\times 1$ vector and the $N/2K\times N/2K$ discrete Fourier transform (DFT) matrix $\boldsymbol{F}_2$ has an $(m,n)$ entry $(1/\sqrt{N/2K})e^{-j2\pi mn/(N/2K)}$, $m,n = 0,1,...,N/2K-1$.

We design the transmit symbol block using the above precoder and hidden pilot with regard to the subcarrier and the antenna index. To support the orthogonality of different antennas' pilot signals for channel prediction, we consider disjoint sets of tones where hidden pilot symbols are included or not in transmit symbol at each antenna. First, we set the $N/2K\times N/2K$ subcarrier index matrix $\boldsymbol{i}_q$ selecting odd and even index vectors, respectively. Here, we assume that an $(N/K-4)\times 1$ information data block for the $k$-th smart device from the $j$-th transmit antenna $\boldsymbol{s}_j^k$ is the i.i.d. zero mean complex Gaussian random vector with covariance $P_s/(N/K-4)I_{N/K-4}$. We also assume that $P_s + P_t = 1$ where $P_t$ denotes the transmit pilot power in one symbol block.

As previously mentioned, to locate disjoint sets of tones, which include hidden pilots or not, in the transmit symbol at each antenna, we design the precoded vector $x_j^k$ as

$$\begin{aligned} x_1^k &= i_1(Ps_{1,1}^k + t) + i_2 Ps_{1,2}^k \\ x_2^k &= i_1 Ps_{2,1}^k + i_2(Ps_{2,2}^k + t), \end{aligned} \tag{4}$$

where $s_{j,1}^k$ and $s_{j,2}^k$ are the odd and even index information data blocks from $s_j^k$, respectively. We then obtain the transmit symbol block $U_j^k$ which is shown as

$$\begin{aligned} U_1^k &= \phi_k(i_1(Ps_{1,1}^k + t) + i_2(Ps_{1,2}^k)) \\ U_2^k &= \phi_k(i_1(Ps_{2,1}^k) + i_2(Ps_{2,2}^k + t)), \end{aligned} \tag{5}$$

where $\phi_k$ is a subcarrier mapping matrix which has the following conditions:

$$\phi_k^H \phi_j = \begin{cases} I_{N/K}, & \text{if } k = j \\ 0_{N/K}, & \text{if } k \neq j \end{cases} \tag{6}$$

Note that we apply equidistantly-located subcarrier mapping which spreads the signal over the total available subcarriers to obtain frequency diversity as much as possible. It is clear from Eq. (5) that the proposed design of hidden pilots imposes good bandwidth efficiency, because we can locate information data over the available MR-OFDM subcarriers and pilots are simply added to certain subcarriers determined by $\phi_k i_1$ or $\phi_k i_2$.

At the $k'$-th smart device's $i$-th receive antenna, an $N/2K \times 1$ vector $r_{i,q}^{k'}$ is selected by the subcarrier demapping matrix $(\phi_{k'} i_q)^H$ for channel estimation and symbol detection, which is given by

$$\begin{aligned} r_{i,1}^{k'} &= (\phi_{k'} i_1)^H F_1 \bar{r}_i^{k'} \\ &= (\phi_{k'} i_1)^H \sum_{j=1}^{2} F_1 H_{ji}^{k'} \left( \sum_{k=1}^{K} F_1^H U_j^k \right) + n_{i,1}^{k'} \\ &= D(\tilde{h}_{1i}^{k',1})(Ps_{1,1}^{k'} + t) + D(\tilde{h}_{2i}^{k',1})(Ps_{2,1}^{k'}) + n_{i,1}^{k'} \end{aligned} \tag{7}$$

$$\begin{aligned} r_{i,2}^{k'} &= (\phi_{k'} i_2)^H F_1 \bar{r}_i^{k'} \\ &= (\phi_{k'} i_2)^H \sum_{j=1}^{2} F_1 H_{ji}^{k'} \left( \sum_{k=1}^{K} F_1^H U_j^k \right) + n_{i,2}^{k'} \\ &= D(\tilde{h}_{1i}^{k',2})(Ps_{1,2}^{k'} + t) + D(\tilde{h}_{2i}^{k',2})(Ps_2^{k'}) + n_{i,2}^{k'} \end{aligned} \tag{8}$$

where $D(\tilde{h}_{ji}^{k',q})$ is an $N/2K \times N/2K$ diagonal channel matrix whose principal diagonal components are the elements of $\tilde{h}_{ji}^{k',q}$, which is the frequency response of a time domain channel $h_{ji}^{k'}$.

## 3. CHANNEL ESTIMATION AND SYMBOL DETECTION

### 3.1 Channel Estimation

At smart devices using the hidden pilot-aided precoding scheme, channel estimation can be carried out by preprocessing received signals in order to reduce the interference between the data and the hidden pilot. The preprocessing is based on the correlation properties of the designed precoder and the hidden pilot. Using the hidden pilot and the inverse DFT matrix for preprocessing, the interference $v_{i,q}^{k'}$ consisting of data symbols is suppressed as

$$\begin{aligned} y_{i,q}^{k'} &= B^H F_2^H r_{i,q}^{k'} \\ &= B^H H_{ji}^{k',q} b + B^H F_2^H n_{i,q}^{k'} + \underbrace{\sum_{j=1}^{2} B^H H_{ji}^{k',q} A s_{j,q}^{k'}}_{v_{i,q}^{k}} \\ &= B^H B h_{ji}^{k'} + \underbrace{v_{i,q}^{k'} + w_{i,q}^{k'}}_{z_{i,q}^{k}} = B^H B h_{ji}^{k'} + z_{i,q}^{k'}, \end{aligned} \tag{9}$$

where $A = F_2^H P$, $b = F_2^H t$, $B$ is an $N/2K \times L$ circulant matrix with the first column $b$, $H_{ji}^{k',q}$ is an $N/2K \times N/2K$ circulant matrix with the first column $\left[h_{ji}^{k'T}, 0, \ldots, 0\right]^T$ and $w_{i,q}^{k'}$ is a modified noise vector, i.e., $w_{i,q}^{k'} = B^H F_2^H n_{i,q}^{k'}$. We have used the fact that $H_{ji}^{k',q} b = B h_{ji}^{k'}$ due to the commutativity of circular

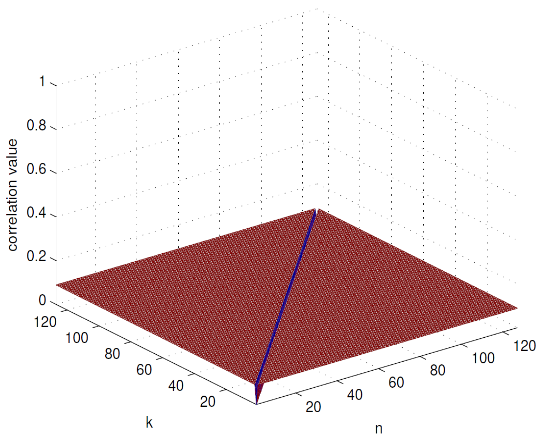


Fig. 2. Periodic crosscorrelation property of the polyphase sequences with k-shifted and n-shifted vectors.

convolution. If we let $A_l$ be a column-wise circulant matrix with the $l$-th column of $A$ as the first column, which we denote as $a_l$, $H_{ji}^{k',q} a_l$ is equivalent to $A_l h^{k'}$.

As depicted in Fig. 2, the polyphase sequence has a good periodic crosscorrelation property. From the figure, we can notice that $B^H A_l$ approaches 0 for all $l$, and thus, we can effectively remove the data interference $v_{i,q}^{k'}$. Then, we can estimate the time domain channel by the linear MMSE channel estimator [14] given by

$$\begin{aligned}\hat{h}_{ji}^{k'} &= E[h_{ji}^{k'} y_{i,q}^{k'\,H}] E[y_{i,q}^{k'} y_{i,q}^{k'\,H}]^{-1} y_{i,q}^{k'} \\ &= E[h_{ji}^{k'} h_{ji}^{k'H}] B^H B (B^H B E[h_{ji}^{k'} h_{ji}^{k'H}] B^H B + E[z_{i,q}^{k'} z_{i,q}^{k'\,H}])^{-1} y_{i,q}^{k'}.\end{aligned} \tag{10}$$

Now, let us define the channel estimation error as $\underline{h}_{ji}^{k'} = h_{ji}^{k'} - \hat{h}_{ji}^{k'}$ and the corresponding mean square error (MSE) can be expressed as

$$\begin{aligned}\sigma_{\underline{h}_{ji}^{k'}}^2 &= tr\,[E[\underline{h_{ji}^{k'}}\,\underline{h_{ji}^{k'H}}]] \\ &= tr\,[E[h_{ji}^{k'} h_{ji}^{k'H}] - E[h_{ji}^{k'} y_{i,q}^{k'H}] E[y_{i,q}^{k'} y_{i,q}^{k'H}]^{-1} E[h_{ji}^{k'} y_{i,q}^{k'H}]] \\ &= tr\,[(E[h_{ji}^{k'} h_{ji}^{k'H}]^{-1} + B^H B (E[v_{i,q}^{k'} v_{i,q}^{k'H}] + \sigma_{w_{i,q}^{k'}}^2 B^H B)^{-1} B^H B)^{-1}],\end{aligned} \tag{11}$$

where $\sigma_{w_{i,q}^{k'}}^2$ is the variance of noise $w_{i,q}^{k'}$. In fact, $B$ shows a good periodic autocorrelation feature, i.e., $B^H B \to cI$ where $c$ is a constant and $I$ is the identity matrix.

### 3.2 Symbol Detection

Using the estimated CSI, the received signal vector $r_{i,q}^{k'}$ is equivalently expressed as

$$r_{i,q}^{k'} = \hat{D}(\tilde{h}_{1i}^{k',q}) P s_{1,q}^{k'} + \hat{D}(\tilde{h}_{2i}^{k',q}) P s_{2,q}^{k'} + \eta_{i,q}^{k'}, \tag{12}$$

where

$$\eta_{i,q}^{k'} = D(\tilde{h}_{ji}^{k'}) t + \sum_{j=1}^{2} \underline{D}(\tilde{h}_{ji}^{k'}) P s_{j,q}^{k'} + n_{i,q}^{k'}. \tag{13}$$

$\hat{D}(\tilde{h}_{ji}^{k'})$ and $\underline{D}(\tilde{h}_{ji}^{k'})$ denote diagonal matrices whose main diagonals are $\hat{h}_{ji}^{k'}$ and $\underline{h}_{ji}^{k'}$, respectively. Since we consider smart devices equipped with two antennas, we can combine two received signal vectors into one signal vector, that is,

$$\underline{r}_{k'}^{q} = \underline{H}_{k'} \underline{s}_{k'}^{q} + \underline{\eta}_{k'}^{q}, \tag{14}$$

where

$$\underline{H_{k'}} = \begin{bmatrix} \hat{D}(\tilde{h}_{11}^{k'}) P & \hat{D}(\tilde{h}_{21}^{k'}) P \\ \hat{D}(\tilde{h}_{12}^{k'}) P & \hat{D}(\tilde{h}_{22}^{k'}) P \end{bmatrix} \tag{15}$$

$$\underline{r_{k'}^{q}} = \left[ r_{1,q}^{k'T}, r_{2,q}^{k'T} \right]^T, \underline{s_{k'}^{q}} = \left[ s_{1,q}^{k'T}, s_{2,q}^{k'T} \right]^T, \underline{\eta_{k'}^{q}} = \left[ \eta_{1,q}^{k'T}, \eta_{2,q}^{k'T} \right]^T.$$

We consider a linear MMSE receiver [12] to detect information data from the received symbols. Then, symbol detection is presented as

$$\begin{aligned}\hat{\underline{s}}_{k'}^{q} &= E[\underline{s}_{k'}^{q} \underline{r}_{k'}^{q\,H}] E[\underline{r}_{k'}^{q} \underline{r}_{k'}^{q\,H}]^{-1} \underline{r}_{k'}^{q} \\ &= \frac{P_s}{\frac{N}{K} - 4} \underline{H}_{k'}^{H} \left( \frac{P_s}{\frac{N}{K} - 4} \underline{H}_{k'} \underline{H}_{k'}^{H} + E[\underline{\eta}_{k'}^{q} \underline{\eta}_{k'}^{q\,H}] \right)^{-1} \underline{r}_{k'}^{q},\end{aligned} \tag{13}$$

where $P_s$ is the total data symbol power in one block. After finishing linear MMSE symbol detection, we can additionally suppress the residual of data interference components by using an iterative algorithm, which further decreases $v_{i,q}^{k'}$, with the help of the detected symbol and the estimated channel. Carrying out the iterative algorithm, a new pre-processed data block $\hat{y}_{i,q}^{k'}$ can be written as

$$\hat{y}_{i,q}^{k'} = y_{i,q}^{k'} - \sum_{j=1}^{2} B^H \hat{H}_{ji}^{k',q} A \hat{s}_{j,q}^{k'} \tag{14}$$

where $\hat{H}_{ji}^{k'}$ is the $N/2K \times N/2K$ circulant matrix with the first column $\left[ \hat{h}_{ji}^{T}, 0, \ldots, 0 \right]^T$. It was observed by numerical simulations that the iterative algorithm for accurate channel estimation converges rapidly within a couple of iterations.

## 4. SIMULATION RESULTS

In this section, the performance of the proposed scheme is evaluated under SUN. For the purpose of comparison, a PSAM scheme is presented as the conventional scheme. As shown in the IEEE 802.15.4g PHY specification [5] for SUN, the total subcarrier number $N$ in MR-OFDM is set to 128 for the SUN-OFDM option 1 and 64 for the option 2. It is assumed that a coordinator transmits data to two smart devices, where each device is equipped with two antennas. The channel is randomly generated at each Monte-Carlo run and is assumed to be Rayleigh with length $L=8$ for OFDM option 1 and $L=4$ for OFDM option 2. Without loss of generality, the number of the disjoint pilot symbols in conventional PSAM is set to the number of channel length.

The channel estimation performance of the proposed scheme based on a hidden pilot is compared to the performance of conventional PSAM in Fig. 3. Here, the pilot power ratio loaded to the hidden pilot is set to 0.7 and the SUN-OFDM option 1 is considered. Note that the analysis of channel estimation error derived in Eq. (11) is similar to the curve obtained with Monte Carlo simulations. In addition, it is shown that the channel estimation performance of the proposed scheme is better than the PSAM scheme in the low SNR region because the proposed one uses a more sufficient number of pilots compared to PSAM. However, in the high SNR, the channel MSE of the proposed scheme is worse since the fact that $B^H A_q \to 0$ is not perfectly satisfied, and thus, it degrades the channel estimation performance. Such a residual interference can be reduced by iteratively updating the detected symbols and the estimated channel, as shown in Fig. 3.

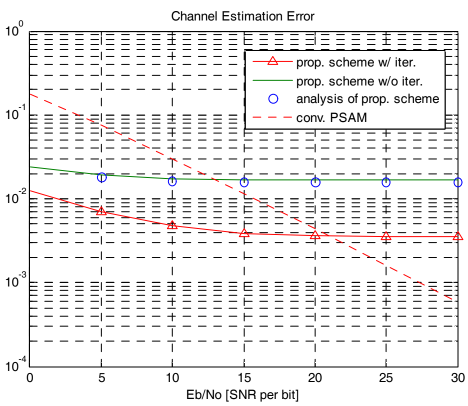


Fig. 3. Performance comparison of channel estimation of the proposed hidden pilot-aided precoding scheme and the conventional PSAM.

Fig. 4 displays the achievable data rate performance of the proposed scheme with regard to the power allocated to the hidden pilot. The power ratio loaded to the hidden pilot varies from 0.3 to 0.7 in the SUN-OFDM option 1 scenario. When SNR is low, the performance of channel estimation has a minor effect on the achievable data rate due to the severe communications condition. However, in the high SNR region, the imperfect channel prediction leads to the notable performance degradation. To obtain high achievable data rate for the high SNR case, the use of pilot power $P_t = 0.7$ is desirable.

The comparison of the achievable data rate between the proposed scheme and the conventional PSAM for the SUN-OFDM option 1 and option 2 are shown in Fig. 5. For both cases, the proposed scheme outperforms the conventional PSAM under overall SNR region. For channel prediction, the proposed scheme does not waste valuable bandwidth, while the PSAM scheme consumes pilot tones which degrades bandwidth efficiency. It can be observed that the proposed scheme provides better achievable data rate in option 1, where a large number of subcarriers are considered, than the one in option 2. Since the precoder in the proposed scheme spreads each symbol over the available frequency domain and achieve a high degree of frequency diversity, the use of a large number of subcarriers, based on the SUN-OFDM option 1,

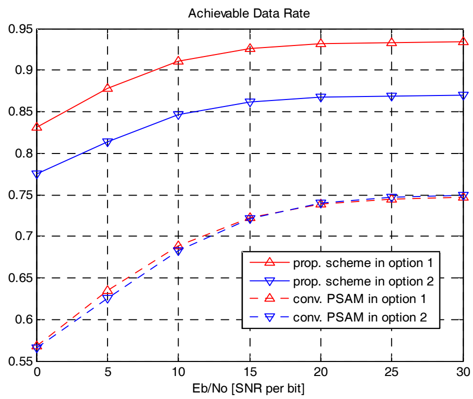


Fig. 4. Achievable data rate comparison for the SUN-OFDM option 1 and option 2.

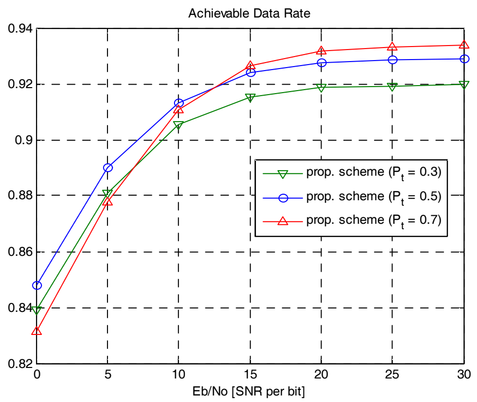


Fig. 5. Achievable data rate for different values of power loaded to the hidden pilot.

results in enhanced performance of achievable data rate.

## 5. CONCLUSION

For the bandwidth efficient communication method in smart utility networks (SUN), a hidden pilot based precoding scheme, which mitigates the mutual interference between the data and pilot symbols, is proposed. The downlink configuration consisting of a coordinator and smart devices, equipped with multiple antennas to provide multi-media data transmissions, is considered. To obtain frequency orthogonality for estimating multiple-antenna channels, we have designed disjoint sets of tones, which include the hidden pilot or not. Since the proposed scheme does not consume bandwidth for channel estimation and provides high frequency diversity, it yields better achievable data rate performance than the conventional PSAM scheme in SUN. The performance gain becomes significant when the use of a large number of sub-carriers, presented as the MR-OFDM option 1 in PHY SUN standard, is considered.

## REFERENCE

[1] NIST, *The Smart Grid Interoperability Standards Roadmap*, 2009.

[2] IEEE 802. 15. 4-2011, *Part 15. 4: Low-Rate Wireless Personal Area Networks*, 2011.

[3] K.-H. Chang and B. Mason, "The IEEE 802.15.4g Standard for Smart Utility Networks," *Proceedings of IEEE 3rd International Conference on Smart Grid Communications (SmartGridComm)*, pp. 476-480, 2012.

[4] D. Choi and I. Chung, "A Study of an Efficient ZigBee Address Assignment Scheme for Home Area Networks of Smart Grid," *Journal of Korea Multimedia Society*, Vol. 16, Issue 5, pp. 566-576, 2013.

[5] J.-S. Kim, H.-Y. Lee, Y.-R. Lee and B.-W. Kim, "Smart Social Grid System using Interactive Sketch Map," *Journal of Korea Multimedia Society*, Vol. 15, Issue 3, pp. 388-397, 2012.

[6] Dr David Hart, *Smart Grid Overview, 15-09-0414-00-wng0*, 2009.

[7] IEEE Standard 802. 15. 4g, *Part 15. 4: Low-Rate Wireless Personal Arae Networks (LR-WPANs) Amendment 3: Physical Layer (PHY) Specifications for Low-Data-Rate, Wireless, Smart Metering Utility Networks*, 2012.

[8] W.G. Jeon, K.H. Paik, and Y.S. Cho, "An Efficient Channel Estimation Technique for OFDM Systems with Transmitter Diversity," *Proceedings of IEEE International Symposium on Personal, Indoor and Mobile Radio Communications*, Vol. 2, pp. 1246-1250, 2000.

[9] S. Adireddy, L. Tong, and H. Viswanathan, "Optimal Placement of Training for Frequency-selective Blockfading Channels," *IEEE Transactions on Information Theory*, Vol. 48, Issue 8, pp. 2338-2352, 2002.

[10] H. Bolcskei, R.W. Heath, and A.J. Paulraj, "Blind Channel Identification and Equalization in OFDM based Multiantenna Systems," *IEEE Transactions on Signal Processing*, Vol. 50, Issue 1, pp. 96-109, 2002.

[11] G.T. Zhou, M. Viberg, and T. McKelvey, "A

First-order Statistical Method for Channel Estimation," *IEEE Signal Processing Letters*, Vol. 10, Issue 3, pp. 57-60, 2003.

[12] M. Ghogho and A. Swami, "Improved Channel Estimation using Superimposed Training," *Proceeding of International Conference on Acoustics, Speech and Signal Processing*, pp. 110-114, 2004.

[13] B.W. Kim, S.Y. Jung, J. Kim, and D.J. Park, "Hidden Pilot based Precoder Design for MIMO-OFDM Systems," *IEEE Communications Letters*, Vol. 12, Issue 9, pp. 657-659, 2008.

[14] J.G. Proakis and M. Salehi, *Digital Communications*, McGraw-Hill Higher Education, New York, 2008.

Byung Wook Kim

He received the B.E. degree from Pusan National University, Pusan, Korea, in 2005 and the M.S. and Ph.D. degrees in Electrical Engineering from KAIST, Daejeon, Korea, in 2007 and 2012, respectively. From 2012 to 2013, he was a senior engineer of Korea Electrotechnology Research Institute (KERI), Changwon, Korea. Currently, he is working as an assistant professor in the School of Electrical and Railway Engineering at Kyungil University. His research interests are in wireless communications, power line communications, visible light communications.